

## Surface Brillouin scattering at high pressure: Application to a thin supported gold film

J. C. Crowhurst, G. R. Hearne, J. D. Comins, A. G. Every, and P. R. Stoddart

*Department of Physics, University of the Witwatersrand, Johannesburg, WITS 2050, South Africa*

(Received 28 June 1999; revised manuscript received 27 September 1999)

Surface Brillouin scattering (SBS) has been used to examine the elastic properties of a supported gold film at high pressure. The velocities of the acoustic modes of a 99 nm thick film have been measured to a pressure of 4.8 GPa, by means of a gem anvil cell with cubic zirconia anvils. A large stiffening of the film has been detected, most clearly revealed by an increase in the value of the  $c_{44}$  elastic constant. The work demonstrates the potential of the SBS technique in high-pressure studies of the elastic properties of opaque materials. [S0163-1829(99)51246-0]

Brillouin scattering (BS) is the inelastic interaction of light with the acoustic phonons of a solid or liquid medium. It has been used for many years to measure the elastic properties of transparent materials at various temperatures and high pressures.<sup>1-3</sup> Since the advent of high contrast Fabry-Perot interferometers, it has developed into a powerful technique for the measurement of the surface acoustic excitations and elastic properties of opaque crystals, films, and layered materials. Such measurements have been extended recently to high temperatures.<sup>4,5</sup> The present work reports a surface Brillouin scattering (SBS) measurement at high pressure using a gem anvil cell.

The SBS technique has been reviewed in detail in the literature.<sup>6</sup> A surface Green's function approach is used to conveniently model the surface dynamics of the sample responsible for the inelastic scattering of the incident light.<sup>7</sup> This formalism has been extended to the present system consisting of a substrate (glass), a thin film (dc-sputtered gold), and a liquid pressure medium (silicone oil).

A modified form of the miniature Merrill-Bassett pressure cell,<sup>8</sup> employing cubic zirconia anvils, was used for these measurements. The anvils and the support structure of the cell were redesigned to permit the laser light beam to be incident obliquely on the sample and to prevent clipping of the collected light cone. The square glass substrate of thickness 90  $\mu\text{m}$  and width 300  $\mu\text{m}$  was mounted on the upper anvil culet and held by epoxy cement around its perimeter (see Fig. 1). A stable sample position is required for the accurate knowledge of the angle of incidence. Also, since high surface quality is essential for SBS, great care was taken during loading to prevent solid contact with the film.

For SBS measured in backscattering, the angle of incidence ( $\theta_i$ ) determines the wave vector of the surface phonons engaged in the scattering, and this information, together with the measured frequency shift ( $\Delta\omega$ ), yields the wave velocity ( $v = \Delta\omega/2k_i \sin(\theta_i)$ , where  $k_i$  is the magnitude of the wave vector of the incident light). The modifications to the cell allowed the measurement of dispersion curves in the form of velocity versus  $\theta_i$  at each pressure. A small rectangular collection aperture ( $\pm 3.5^\circ$ ) was used to improve resolution and accuracy<sup>9</sup> while preserving an adequate signal to noise ratio owing to the excellent sensitivity of the silicon avalanche diode detector. The use of a microscope proved essential in focusing and positioning the laser beam in the

cell cavity to within the same 100  $\mu\text{m}$  spot of the film surface for each measurement. The SBS spectrometer employed a Sandercock 3+3 pass tandem Fabry-Perot interferometer.<sup>10</sup>

The particular choice of sample for this initial SBS experiment at high pressure was made for several reasons. High-pressure studies of the elastic properties of bulk solids by ultrasonics are well established.<sup>11</sup> The complementary technique of SBS is one of the very few methods available to examine opaque thin films less than a few hundred nanometers thick.<sup>12</sup> Owing to the anticipated reduction in signal strength from inside the cell, it was considered advisable to select a material with a high scattering efficiency and a detailed thin-film SBS spectrum [Fig. 2(a)]. Gold was chosen for this property and for its chemical inertness. A depth profile study by x-ray photoelectron spectroscopy (XPS) revealed a pure film with minimal or no surface or interface contamination. XPS combined with a step profile measurement set the thickness of the film at  $99 \pm 3$  nm.<sup>13</sup> X ray-diffraction measurements confirmed the preferred orientation of the crystallites, with the [111] direction normal to the substrate and with the two orthogonal axes randomly oriented. The average of the calculated Voigt and Reuss elastic constants for the resulting transversely isotropic<sup>14,15</sup> system is listed in Table I together with the cubic single-crystal values.

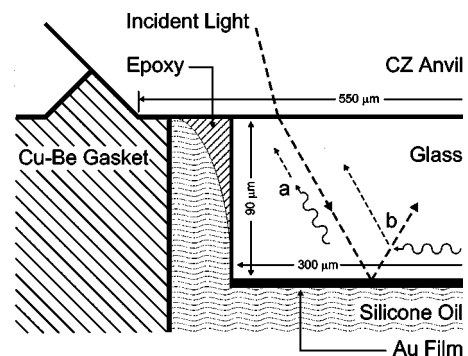


FIG. 1. Schematic of cell cavity showing sample orientation and scattering configuration. The small dashes represent the path of the collected light corresponding to the backscatter *a*, and platelet geometries *b*. The scattering can be observed for light incident on either side of the gold film, since both are corrugated by the gold surface modes. The glass side was chosen for the reasons given in the text.

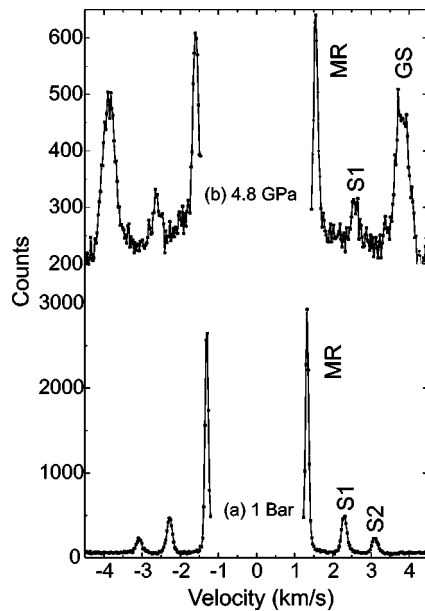


FIG. 2. (a) Measured SBS spectrum from gold film/air interface at  $\theta_i=45^\circ$ , showing the modified Rayleigh (MR) and Sezawa modes (S1, S2). (b) The SBS spectrum from the glass/gold film interface at 4.8 GPa and  $\theta_i=50.4^\circ$ . GS is the glass shear mode. To obtain the frequency shift, the peaks were fitted with a Lorentzian curve and baseline combination.

The scattering configuration within the cell, because of the reflective film, was a combination of the backscatter and ‘‘platelet’’<sup>16</sup> geometries (Fig. 1). This resulted in several distinct contributions to the Brillouin spectrum from the surrounding materials. Depending on the nature of the mode and the material, these could be of similar intensity or orders of magnitude greater than the signals of interest. Successful observation was thus occasionally difficult. On the other hand the configuration allowed the simultaneous measurement of the glass compressional and shear frequencies. Comparison of the frequencies of the compressional mode corresponding to the two geometries yielded the glass refractive index. Both elastic moduli of the substrate (i.e.,  $c_{11}$  and  $c_{44}$ ) could then be calculated. This was useful because the acoustic behavior of a surface region is in general intimately dependent on the elastic properties of the upper (sample or substrate) and lower (pressure medium) materials. Thus it is in principle necessary to acquire and interpret not just one set of Brillouin frequencies as in the case of scattering from

TABLE I. Elastic stiffness constants of gold film at ambient pressure and at 4.8 GPa. Values in GPa.

	$c_{11}$	$c_{12}$	$c_{13}$	$c_{33}$	$c_{44}$
Single-crystal values <sup>a</sup>	190	161	-	-	42.3
Voigt/Reuss [111] average	212	154	142	225	21.3
[111] fit to ambient data	212 <sup>b</sup>	154 <sup>b</sup>	142 <sup>b</sup>	199	21.3
[111] fit to 4.8 GPa data <sup>c</sup>	212 <sup>b</sup>	154 <sup>b</sup>	142 <sup>b</sup>	282	44

<sup>a</sup>Reference 21.

<sup>b</sup>Not varied in fit.

<sup>c</sup>The measured high-pressure value of the glass shear modulus (36.5 GPa) was used in these calculations.

TABLE II. Measured SiO<sub>2</sub> content, refractive index, density, and elastic moduli of glass substrate under ambient conditions.

SiO <sub>2</sub> (%)	$n$	$\rho(\text{g cm}^{-3})$	$c_{44}$ (GPa)	$c_{11}$ (GPa)
64.1 <sup>a</sup>	1.52	2.51	29.4	80.8

<sup>a</sup>Determined using x-ray fluorescence.

transparent samples at high pressure, but two, or even three if the sample takes the form of a supported thin film.

We found it prudent to choose a combination of materials that minimizes this dependence. The observed ambient pressure spectrum of Fig. 2(a) contains the responses due to the surface modes of the gold film. The dominant peak is due to the modified Rayleigh surface mode (MR). Since the substrate shear velocity was very much larger than that of the film the others are identified as first- and second-order Sezawa guided modes.<sup>7</sup> The Green’s function method discussed above shows that for a large range of bulk modulus, a liquid pressure medium (such as silicone oil<sup>17</sup>) has little effect on the frequency of the surface modes. On the other hand, the behavior with pressure of a solid substrate, such as glass, has a somewhat more important effect mainly due to changes in its shear modulus. As discussed below, the observed decrease in the velocity of the MR mode at around 1 GPa, for example, can be attributed to the observed softening in the glass substrate. The amorphous nature of the glass, however, was a distinct practical advantage since knowledge of the azimuthal angle was not required in the evaluation of the SBS results. It should also be noted that the calculated effect of the substrate and even of a pressure-induced solidification of the silicone oil on the velocity of the film-guided Sezawa modes was minimal, at least to the pressure reported here. We conclude therefore that the large increase observed in the velocity of the first Sezawa mode was indicative of real changes in the elastic properties of the gold film at high pressure.

For purposes of comparison SBS and BS measurements were made on the sample before pressurization [Tables I and II and Fig. 2(a)]. The Voigt/Reuss elastic constants of Table I for the strongly textured film were used as initial estimates in a least-squares fitting procedure to the ambient pressure dispersion curves (Fig. 3). Since contributions from  $c_{11}$ ,  $c_{13}$ , and  $c_{33}$  were similar, only two parameters were treated as free in the calculation,<sup>15,18</sup> namely  $c_{33}$  and  $c_{44}$ . The fit was excellent and coincided with a decrease in  $c_{33}$  of about 12% from the initial estimate. The observation that a fit assuming isotropic symmetry was significantly less successful demonstrates the importance of the film texture. These results can be compared with those of Grimsditch *et al.*<sup>19</sup> The value for  $c_{44}$  found in the latter reference is about 13% less than that reported here. This discrepancy may be related to the different deposition method used to produce the film in the two cases and to the degree of film texture.

The observed velocity of the MR mode for a single incident angle versus pressure is shown in Fig. 4. Also shown are the calculated velocities corresponding to the observed changes in the glass moduli only. The reduction near 1 GPa is consistent with other observations of the behavior of certain glasses in the low-pressure region.<sup>20</sup> The corresponding calculated and observed first Sezawa velocities at the pres-

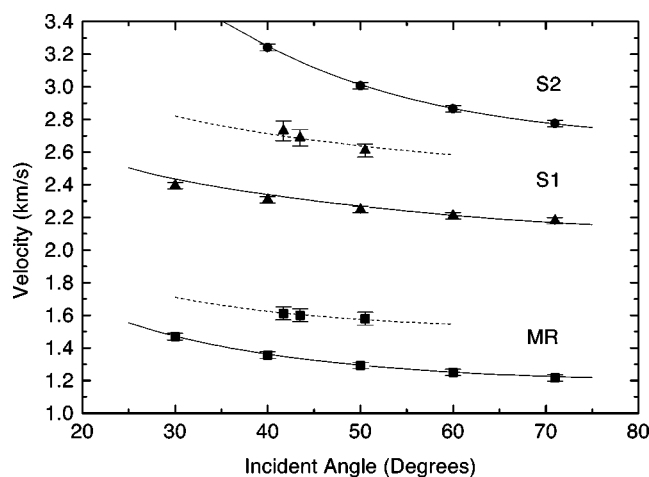


FIG. 3. Computed dispersion curves for the gold film data (symbols) at ambient pressure (continuous lines) and 4.8 GPa (dashed lines).

ures at which these modes were observed are also plotted. The increasing separation of the values at high pressure shows that the increase in the film mode velocities is not only due to changes in the elastic properties of the substrate. A fit to the data at a pressure of 4.8 GPa [e.g., Fig. 2(b)] yields the dashed dispersion curves in Fig. 3. Although the second Sezawa mode was consistently hidden by the glass transverse peak, an increase in the velocity of the other two modes is evident. The corresponding change in the elastic constants  $c_{33}$  and  $c_{44}$ , calculated from the high-pressure dispersion curves of Fig. 3, is large (Table I). There is of course no physical reason to assume an increase in two constants only. Changes in  $c_{11}$  and  $c_{13}$  would be compensated by a smaller increase in  $c_{33}$  (but not  $c_{44}$ , which is largely decoupled from the other three constants). A likely explanation for the large change in  $c_{44}$  hinges on the mismatch between the glass and gold bulk moduli. The large compressibility of the glass results in a large induced compressional stress in the plane of the film at high pressure. This is in agreement with the observed recurrent delamination of the film above 5 GPa. SBS measurements performed on the recovered and intact 4.8 GPa sample did not suggest any permanent changes in the film constants. This may be in accordance with the observed elastic behavior of the substrate. A quantitative analysis of the effect will be reported elsewhere.

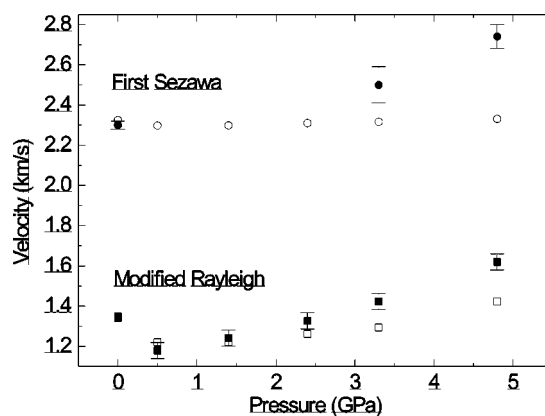


FIG. 4. Measured modified Rayleigh and first Sezawa velocities (solid squares and circles, respectively), and corresponding calculated values (open squares and circles, respectively) assuming only the observed changes of the glass substrate. For all points  $\theta_i = 42^\circ$ .

In conclusion, SBS measurements have revealed a large increase in the effective stiffness of a glass supported polycrystalline gold film at high pressure. This is most clearly revealed by the enhancement in the value of the gold  $c_{44}$  elastic constant. The work has illustrated the potential of SBS to measure the elastic properties of supported opaque thin films at high pressure. Future developments may include the use of diamond anvils to greatly increase the pressure range and an extension to high temperatures; as such the technique would provide an alternative to the ultrasonic methods using multianvil presses.<sup>11</sup> Practical applications include the assessment of mechanical performance of hard and ultrahard coatings at elevated external stress and the study of bulk opaque minerals under deep-Earth conditions.

The authors would like to thank A. L. Ruoff for suggesting the mechanism responsible for the induced stress in the film at high pressure, as well as M. Grimsditch and M. H. Manghnani for valuable discussion. We would also like to thank J. van der Vyfer (Microchip Corporation) for preparing the gold films and substrates, and P. Huebscher for fabricating the CZ anvils. We express our gratitude to the National Research Foundation of South Africa (formerly the Foundation for Research Development) for financial support of this work.

<sup>1</sup>J. Xu and M. H. Manghnani, Phys. Rev. B **45**, 640 (1992).

<sup>2</sup>A. Polian and M. Grimsditch, Phys. Rev. B **27**, 6409 (1983).

<sup>3</sup>A. Polian and M. Grimsditch, Phys. Rev. B **47**, 13 979 (1992).

<sup>4</sup>P. R. Stoddart, J. D. Comins, and A. G. Every, Phys. Rev. B **51**, 17 574 (1995).

<sup>5</sup>W. Pang, P. R. Stoddart, J. D. Comins, A. G. Every, D. Pietersen, and P. J. Marais, Int. J. Refract. Hard Met. **15**, 179 (1997).

<sup>6</sup>P. Mutti, C. E. Bottani, G. Ghislotti, M. Beghi, G. A. D. Briggs, and J. R. Sandercock, in *Surface Brillouin Scattering-Extending Surface Wave Measurements to 20 Ghz*, edited by A. Briggs, Advances in Acoustic Microscopy Vol. 1 (Plenum, New York, 1995), p. 249.

<sup>7</sup>X. Zhang, J. D. Comins, A. G. Every, P. R. Stoddart, and W. Pang, Phys. Rev. B **58**, 13 677 (1998).

<sup>8</sup>E. Sterer, M. P. Pasternak, and R. D. Taylor, Rev. Sci. Instrum. **61**, 1117 (1990).

<sup>9</sup>P. R. Stoddart, J. C. Crowhurst, A. G. Every, and J. D. Comins, J. Opt. Soc. Am. B **15**, 2481 (1998).

<sup>10</sup>J. R. Sandercock, in *Light Scattering in Solids III*, edited by M. Cardona and G. Güntherodt, Topics in Applied Physics Vol. 51 (Springer, Berlin, 1982), p. 173.

<sup>11</sup>R. C. Liebermann and B. Li, in *Ultrahigh-Pressure Mineralogy: Physics and Chemistry of the Earth's Deep Interior*, edited by R. J. Hemley, Reviews in Mineralogy Vol. 37 (Mineralogical Soc.

- Am., Washington, DC, 1998), p. 459.
- <sup>12</sup>M. G. Beghi, C. E. Bottani, P. M. Ossi, T. A. Lafford, and B. K. Tanner, *J. Appl. Phys.* **81**, 672 (1997).
- <sup>13</sup>Elastic continuum theory is still applicable to this thickness; see, for example, Ref. 21.
- <sup>14</sup>A. Moreau, J. B. Ketterson, and B. Davis, *J. Appl. Phys.* **68**, 1622 (1990).
- <sup>15</sup>R. Jorna, D. Visser, V. Bortolani, and F. Nizzoli, *J. Appl. Phys.* **65**, 718 (1988).
- <sup>16</sup>C. H. Whitfield, E. M. Brody, and W. A. Bassett, *Rev. Sci. Instrum.* **47**, 942 (1976).
- <sup>17</sup>D. D. Ragan, D. R. Clarke, and D. Schiferl, *Rev. Sci. Instrum.* **67**, 494 (1996).
- <sup>18</sup>G. Carlotti, D. Fioretto, G. Socino, B. Rodmacq, and V. Pelosin, *J. Appl. Phys.* **71**, 4897 (1992).
- <sup>19</sup>M. Grimsditch, R. Bhadra, and I. K. Schuller, *Phys. Rev. Lett.* **58**, 1216 (1987).
- <sup>20</sup>M. H. Manghnani (private communication).
- <sup>21</sup>B. Hillebrands, P. Baumgart, R. Mock, G. Güntherodt, and P. S. Bechtold, *J. Appl. Phys.* **58**, 3166 (1985).